

The Chemical Composition of Ryugu: Prospects as a Reference Material for Solar System Composition

Tetsuya Yokoyama^{1*}, Nicolas Dauphas², Ryota Fukai³, Tomohiro Usui³, Shogo Tachibana⁴, Maria Schönbächler⁵, Henner Busemann⁵, Masanao Abe³, and Toru Yada³

¹ Department of Earth & Planetary Sciences, Tokyo Institute of Technology, Japan

² Origins Lab, Department. of the Geophysical Sciences and Enrico Fermi Institute, The University of Chicago, USA

³ Astromaterials Science Research Group, ISAS, JAXA

⁴ Department of Earth and Planetary Science, University of Tokyo, Japan

⁵ Institut für Geochemie und Petrologie, ETH Zürich, Switzerland

*Corresponding author E-mail: tetsuya.yoko@eps.sci.titech.ac.jp

Abstract

The Hayabusa 2 spacecraft sampled ~5.4 g of asteroid material from the Cb-type asteroid Ryugu. Initial analysis of the Ryugu materials revealed a mineralogical, chemical, and isotopic kinship to the CI chondrites. The pristine nature of Ryugu makes the returned samples ideal for constraining the composition of the Solar System. However, some elements (e.g., P, Ca, Mn, and rare earth elements) show large relative dispersions compared to the other elements in the returned materials studied so far, most likely due to the presence of aqueously formed secondary minerals (e.g., carbonates, phosphates) in Ryugu. Therefore, the estimation of the Solar System composition using currently available Ryugu data is challenging due to the so-called “nugget effect” of carbonates, phosphates, and possibly other accessory minerals. The nugget effect can be mitigated by analyzing a homogenized, relatively large amount of sample. We estimate that for ~0.1 g of Ryugu sample, the dispersion (2SD) of the bulk Mn/Cr and Rb/Sr ratios are $\pm 13\%$ and $\pm 15\%$, respectively, while they will be improved to be better than $\pm 5\%$ for ~1 g of homogenized Ryugu sample. To further constrain the Solar System composition and to evaluate if previous estimates based on CI chondrites stored in museums for decades to centuries are reliable, it is strongly recommended to determine the chemical and isotopic compositions of Ryugu using a homogenized sample prepared from relatively large (~1 g) returned material. Determining Ryugu reference compositions will be used by multidisciplinary communities, including Earth and planetary sciences, astronomy, physics, and chemistry.

1. Introduction

Accurate determination of the composition of the Solar System is critical for advancing our understanding of the formation and evolution of the Solar System including its planets and small bodies, the chemical evolution of galaxies, and the processes that govern the origin of the elements. Precise dating of meteorites and their constituents, coupled with theoretical modeling of planet formation, has revealed that the Solar System began with the gravitational collapse of a molecular cloud core at about 4.6 billion years ago (e.g., Amelin *et al.*, 2002; Connelly *et al.*, 2012). The chemical composition of the Solar System provides valuable information about the initial conditions of the solar nebula from which the Solar System formed and evolved into planets,

moons, asteroids, and comets. It also serves as an important baseline for studying the chemical composition of other stars and exoplanets, as well as the interstellar medium and galaxies. Furthermore, the chemical composition of the Solar System integrates materials contributed by various stellar objects that existed before the birth of the Solar System, helping to elucidate the nucleosynthetic mechanisms that produced the elements (Yokoyama and Tsujimoto, 2021).

The elemental abundances of the Sun have been used to represent the chemical composition of the Solar System, since more than 99% of the mass of the Solar System is locked up in the Sun. There are several ways to determine the elemental abundances of the Sun, and each method provides complementary information about the composition of the Sun. One of the most

important and direct methods for determining the elemental abundances of the Sun is spectroscopy, which involves the analysis of dark lines at specific wavelengths corresponding to the absorption of light by atoms in the solar photosphere. Spectroscopy of the solar photosphere in determining the elemental abundances of the Sun has several difficulties, including mixing of multiple spectral lines, uncertainties in the solar atmospheric models that describe the physical conditions of the Sun, the stratification of elemental abundances in the upper and lower layers of the solar atmosphere, and the analysis of weak lines for extremely low-abundance elements. Despite these difficulties, the abundances of 68 elements in the solar photosphere are reported with uncertainties of 10–20% for about two-thirds of these elements, whereas the remainder have uncertainties >20%, specifically for minor elements and volatiles (Lodders, 2021). Helioseismology, which observes the oscillations and vibrations of the Sun's surface and interior, is an alternative approach to determining the elemental abundances of the Sun. Although helioseismology is an indirect method of inferring the chemical composition of the Sun, it provides data for helium that cannot be determined by spectroscopy (Lodders, 2020).

Another robust method for determining the chemical composition of the Solar System is the measurement of chondritic meteorites, which are fragments of asteroids that did not melt after accretion in the early Solar System (Scott and Krot, 2014). Of all the chondrites, which account for about 90% of the >70,000 meteorites discovered on Earth to date (Meteoritical Bulletin Database: <https://www.lpi.usra.edu/meteor/metbull.php>), the Ivuna-type (CI) carbonaceous chondrites have been perceived as a unique group of meteorites with a chemical composition similar to that of the solar photosphere except for some elements (e.g., noble gases, H, C, N, and Li). A major advantage of CI chondrite measurements is that not only elemental abundances but also isotopic compositions can be measured directly in the laboratory with high precision. Most notably, the data obtained estimates the composition of the Solar System at about 4.6 billion years ago, which does not necessarily agree with the current composition of the Sun for some elements as determined by spectroscopy and helioseismology. A severe problem associated with the measurement of meteorites is the unavoidable contamination of terrestrial materials when a meteor enters the Earth and hits the ground, and during the long-term storage of meteorites in museums. Additionally, CI chondrites are extremely rare, only five witnessed fall CIs have been collected so

far (Alais, Ivuna, Orgueil, Revelstoke, and Tonk). Of note, a recent study concluded that the elemental abundances of Ivuna, Alais, and Tonk agree well with the results of the Orgueil analyses, with only a few exceptions, indicating that all CI chondrites have essentially the same fractions of the fundamental cosmochemical components (Palme and Zipfel, 2022). The authors concluded that the CI composition is a well-defined entity representing the non-gaseous compositions of the solar nebula and photosphere of the Sun.

Sample return missions are superior to meteorite analysis in that samples can be collected with no or a minimum of contamination from well-documented extraterrestrial objects. The Japan Aerospace Exploration Agency's (JAXA) Hayabusa 2 spacecraft, targeting the Cb-type asteroid (162173) Ryugu, sampled ~5.4 g of asteroidal material and returned the samples to Earth in December 2020 (Tachibana *et al.*, 2022; Yada *et al.*, 2022). These samples were collected during the two landing sequences on the asteroid Ryugu. During the first touch-down operation (TD1), samples were collected from the asteroid surface and stored in sample Chamber A, while the other samples stored in sample Chamber C were collected from the vicinity of an artificial crater created by the small carry-on impactor during the second touch-down operation (TD2). The TD1 and TD2 samples were stored and handled separately at the JAXA curation facility (Yada *et al.* 2022).

Initial analyses of the Ryugu materials in both chambers revealed a mineralogical and chemical kinship to the CI chondrites (Nakamura *et al.*, 2022; 2023; Yokoyama *et al.*, 2023a) with a composition similar to the solar photosphere for non-volatile elements (Lodders, 2021). Tantalum stands out with a large excess in the Ryugu samples, but this is due to contamination from the Ta projectile used for sampling (Nakamura *et al.*, 2022; Yokoyama *et al.*, 2023a). Isotopic analyses of Ryugu materials showed that Ryugu and CI chondrites presumably originated from the outskirts of the Solar System (Hopp *et al.*, 2022; Kawasaki *et al.*, 2022; Paquet *et al.*, 2023). The pristine nature of Ryugu, except for Ta, makes the returned samples ideal for constraining the composition of outer Solar System material, which is considered a proxy for the composition of the Solar System.

The present study summarizes the elemental abundances of Ryugu bulk samples published to date, evaluates the compositional variability, and compares the results with those of CI chondrites. In particular, the influence of the heterogeneous distribution of secondary

minerals formed during aqueous alteration of the parent body is discussed to assess the dispersion of elemental ratios among different Ryugu fragments. We then demonstrate the scientific need for a consortium to determine the representative elemental abundances and isotopic compositions of Ryugu using a relatively large amount of homogenized powder sample. The data obtained throughout the activity of the consortium should be used to complement the scientific objectives of the Hayabusa2 mission, including investigations of (1) the evolution from a planetesimal to a near-Earth asteroid, (2) the possible destruction and accumulation of a rubble-pile body formed from a larger, aqueously altered parent planetesimal, (3) the diversification of organic materials through interactions with minerals and water in a planetesimal, and (4) the chemical heterogeneity in the early Solar System (Tachibana *et al.*, 2014). Furthermore, we anticipate the potential of the Ryugu sample as a new reference material of the Solar System, which will be beneficial for multidisciplinary communities in various scientific fields, extending beyond the scope of the Hayabusa2 project.

2. Summary of the reported Ryugu data

2.1. Elemental abundances of bulk Ryugu samples

Six previous studies have measured elemental abundances of bulk Ryugu samples using different approaches. Yokoyama *et al.* (2023a) quantified the abundances of 66 elements in the Ryugu samples by X-ray fluorescence (XRF), inductively coupled plasma mass spectrometry (ICP-MS), thermogravimetric analysis coupled with mass spectrometry (TG-MS), and combined analyses of pyrolysis and combustion. In the XRF analysis, 33 mg of an aggregate Ryugu sample C0108 was first powdered, of which 24 mg was set in an acrylic sample cell to determine 22, 17, and 18 elements by wavelength dispersive (WD), energy dispersive (ED), and high energy (HE) XRF, respectively. The powdered sample C0108 in the cell was retrieved after the XRF measurements, and acid digested to a homogeneous solution for ICP-MS measurements of 54 elements. Additionally, 24 mg of a powdered sample A0106-A0107, prepared from a mixed aggregate of A0106 (1.6 mg) and A0107 (27 mg), was acid digested into a homogeneous solution for ICP-MS analysis. Therefore, these elemental abundances represent the bulk chemical composition in a relatively large size (24 mg) of Ryugu

samples. On the other hand, two ~1 mg aliquots of A0040 were used in the TG-MG and pyrolysis measurements to determine the abundances of H and C.

Nakamura *et al.* (2022) examined 16 individual Ryugu particles (A0022, A0033, A0035, A0048, A0073, A0078, A0085, C0008, C0019, C0027, C0039, C0047, C0053, C0079, C0081, and C0082) for comprehensive geochemical analyses, ranging in size from 1.2 to 3.7 mm (largest dimension) and weight from 0.7 to 10.0 mg. For the determination of elemental abundances, an aliquot from each particle (0.33–3.3 mg) was separated and further divided into up to 8 portions to determine the abundances of different groups of elements. Exceptionally, two aliquots (0.40 and 0.18 mg) were taken from one particle C0053 to duplicate the measurements. Using these aliquots, up to 66 elements were measured by ICP-MS, while the abundances of Ne and H, C, and N were determined by noble gas mass spectrometry (noble gas MS) and isotope ratio mass spectrometry (IR-MS), respectively. The abundance of Si was not measured directly, but calculated from the Si/Mg ratio obtained by SEM-EDS elemental mapping of the entire particle cross-section prepared by an ultramicrotome, and the Mg abundance determined by ICP-MS analysis. In contrast to Yokoyama *et al.* (2023a), the elemental abundances determined by Nakamura *et al.* (2022) are determined in separated small aliquots and thus do not necessarily represent the bulk chemical composition of individual particles.

Ito *et al.* (2022) measured the abundances of 20 elements in two Ryugu particles (1.06 mg of A0098; 0.65 mg of C0068) by instrumental neutron activation analysis (INAA). Okazaki *et al.* (2023) determined noble gas, C, and N abundances in two Ryugu samples (A0105 and C0106) by mass spectrometry. Naraoka *et al.* (2023) and Oba *et al.* (2023) measured the abundances of H, C, N, O, and S in Ryugu samples A0106 and C0107 by elemental analyzer (EA)-IRMS, respectively. In total, the six previous studies mentioned above measured the abundances of 79 elements. Lodders (2021) reported the abundances of 83 elements as representative for CI chondrites. The elements that have not yet been measured for bulk Ryugu samples are F, Br, I, and Hg.

In the six previous studies, different methods were applied to different batches of samples, some of which were relatively small (e.g., <1 mg) and thus potentially chemically heterogeneous (see below). This makes it difficult to accurately determine “bulk” Ryugu elemental abundances using established statistical protocols performed by previous compilation studies on reference

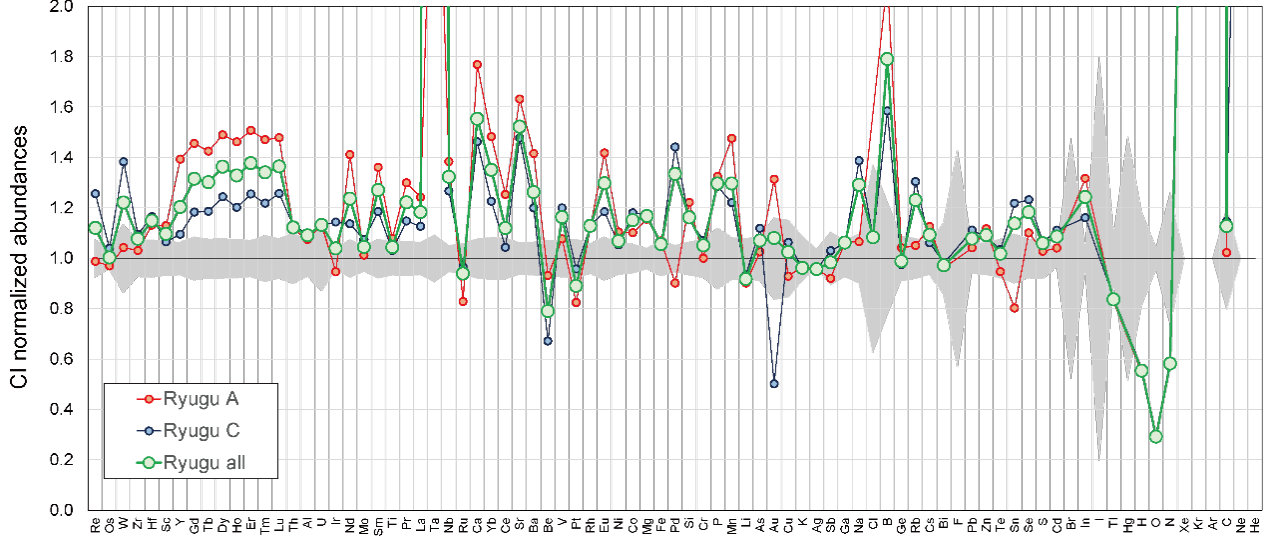


Fig. 1 CI-normalized elemental abundances in bulk Ryugu samples determined by six previous studies (Ito *et al.*, 2022; Nakamura *et al.*, 2022; Naraoka *et al.*, 2023; Oba *et al.*, 2023; Okazaki *et al.*, 2023; Yokoyama *et al.*, 2023a). CI chondrite data were taken from Lodders (2021).

materials (e.g., Jochum *et al.*, 2016). Here, we present the current best estimates for the Ryugu elemental abundances with a straightforward approach that calculates the averages of the reported data, taking into account the measured sample weights;

$$C = \frac{\sum C_i m_i}{\sum m_i} \quad (1)$$

where C_i and m_i are the mass fraction and weight, respectively, of the i -th measurement of a target element. **Table 1** summarizes the results of the estimated bulk Ryugu abundances for 79 elements in TD1, TD2, and all samples. The uncertainties σ_C of the estimated abundances were calculated by propagating the uncertainties associated with $C(X)_i$ and m_i using

$$\sigma_C = C \sqrt{\frac{\sum C_i^2 \sigma_{m_i}^2 + \sum m_i^2 \sigma_{C_i}^2}{(\sum C_i m_i)^2} + \frac{\sum \sigma_{m_i}^2}{(\sum m_i)^2}} \quad (2).$$

Figure 1 shows the estimated elemental abundances of bulk Ryugu samples normalized to CI chondrite values (Lodders, 2021). As discussed in previous studies, the Ryugu elemental abundances show close agreement with CI chondrites from refractory to volatile elements, with slight excesses in most elements, possibly due to the depletion of H_2O in Ryugu compared to CI chondrites (Yokoyama *et al.*, 2023a).

2.2. Isotopic abundances of bulk Ryugu samples

The above six previous studies measured the bulk isotopic compositions of various elements in the Ryugu samples used in the measurement of bulk elemental abundances (Ito *et al.*, 2022; Nakamura *et al.*, 2022; Naraoka *et al.*, 2023; Oba *et al.*, 2023; Okazaki *et al.*, 2023; Yokoyama *et al.*, 2023a). These include H, C, N, O, S, Ca, Ti, Cr, and noble gas elements (He, Ne, Ar, Kr, and Xe). Additional measurements of bulk isotopic compositions were performed using the same sample aliquots described in Yokoyama *et al.* (2023a) for Mg (Bizzarro *et al.*, 2023), K (Hu *et al.*, 2024), Ca (Moynier *et al.*, 2022), Cr and Ti (Yokoyama *et al.*, 2023b), Fe (Hopp *et al.*, 2022), Cu and Zn (Paquet *et al.*, 2023), Zr (Schönbächler *et al.*, in revision), Mo (Nakanishi *et al.*, 2023), and Sm-Nd (Torrano *et al.*, 2024). Similar to the results of elemental abundances, most of the isotopic compositions in bulk Ryugu samples were generally consistent with those of CI chondrites, suggesting that the source materials of Ryugu and CIs share a common genetic heritage. In particular, Ryugu and CIs have indistinguishable $^{54}\text{Fe}/^{56}\text{Fe}$ ratios, which are different from the other carbonaceous chondrite (CC) and non-carbonaceous (NC) chondrite groups (Hopp *et al.*, 2022). A plausible explanation by the authors is that the parent bodies of Ryugu and CIs were deflected into the main belt from the outer Solar System by excitation of Uranus and Neptune, while other CC bodies formed in more inner regions of the Solar System, near Jupiter and Saturn. In contrast, $^{54}\text{Cr}/^{52}\text{Cr}$ ratios in Ryugu samples with masses <25 mg showed a variation exceeding the

Table 1 Elemental abundances of bulk Ryugu samples

Z	E	Ryugu (TD1)			Ryugu (TD2)			Ryugu (All)			CI (Lodders 2021)	
		$\mu\text{g/g}$	2σ	n	$\mu\text{g/g}$	2σ	n	$\mu\text{g/g}$	2σ	n	$\mu\text{g/g}$	2σ
1	H	10098	± 796	8	10443	± 121	8	10291	± 357	16	18600	± 3440
2	He	0.189	± 0.006	12	0.0252	± 0.0010	5	0.155	± 0.005	17	0.00917	± 0.00000
3	Li	1.36	± 0.09	8	1.41	± 0.07	11	1.38	± 0.06	19	1.51	± 0.12
4	Be	0.0205	± 0.0052	6	0.0148	± 0.0018	11	0.0174	± 0.0026	17	0.0220	± 0.0016
5	B	1.57	± 0.04	4	1.18	± 0.02	7	1.33	± 0.02	11	0.744	± 0.172
6	C	42185	± 3956	9	47337	± 2711	12	46516	± 2365	21	41300	± 8400
7	N	1473	± 26	9	1439	± 24	11	1454	± 17	20	2500	± 660
8	O	129300	± 4000	1	134000	± 10000	1	132264	± 6477	2	453840	± 20000
9	F										92.0	± 40.0
10	Ne	0.0141	± 0.0021	19	0.000770	± 0.000059	15	0.00650	± 0.00090	34	0.000180	± 0.000000
11	Na	5433	± 79	9	7072	± 94	14	6585	± 70	23	5100	± 500
12	Mg	109859	± 1082	9	111562	± 577	14	111056	± 517	23	95170	± 4000
13	Al	8986	± 112	9	9183	± 67	14	9125	± 58	23	8370	± 600
14	Si	131505	± 1808	7	124019	± 702	12	125110	± 656	19	107740	± 7200
15	P	1295	± 37	8	1256	± 21	13	1267	± 18	21	978	± 120
16	S	55059	± 384	5	56998	± 307	10	56750	± 272	15	53600	± 4400
17	Cl				776	± 22	1	776	± 22	1	717	± 270
18	Ar	0.0608	± 0.0016	12	0.101	± 0.003	6	0.0733	± 0.0015	18	0.00133	± 0.00000
19	K	522	± 15	9	516	± 10	14	518	± 8	23	539	± 48
20	Ca	15629	± 288	9	12919	± 137	13	13728	± 129	22	8840	± 700
21	Sc	6.58	± 0.24	9	6.21	± 0.06	12	6.39	± 0.12	21	5.83	± 0.40
22	Ti	485	± 5	5	463	± 10	10	469	± 8	15	450	± 30
23	V	57.7	± 1.7	9	64.3	± 3.7	14	62.3	± 2.6	23	53.6	± 4.0
24	Cr	2609	± 35	6	2793	± 25	11	2740	± 20	17	2610	± 200
25	Mn	2796	± 30	9	2313	± 19	14	2456	± 16	23	1896	± 160
26	Fe	198268	± 1788	9	194842	± 1066	14	195860	± 919	23	185620	± 13000
27	Co	559	± 7	9	599	± 8	13	584	± 6	22	508	± 30
28	Ni	12084	± 115	9	11524	± 63	14	11690	± 56	23	10950	± 700
29	Cu	121	± 3	8	138	± 2	13	133	± 2	21	130	± 20
30	Zn	347	± 7	9	336	± 4	15	339	± 4	24	311	± 20
31	Ga	10.0	± 0.4	9	10.0	± 0.7	13	10.0	± 0.5	22	9.45	± 0.70
32	Ge	34.8	± 0.6	3	32.5	± 1.4	4	33.0	± 1.1	7	33.4	± 3.0
33	As	1.81	± 0.04	5	1.98	± 0.05	5	1.89	± 0.03	10	1.77	± 0.16
34	Se	22.4	± 0.8	5	25.1	± 0.7	6	24.1	± 0.5	11	20.4	± 1.6
35	Br										3.77	± 1.80
36	Kr	0.000177	± 0.000002	12	0.000246	± 0.000005	5	0.000191	± 0.000002	17	0.0000522	± 0.0000000
37	Rb	2.33	± 0.06	8	2.89	± 0.47	13	2.73	± 0.34	21	2.22	± 0.18
38	Sr	12.7	± 0.2	8	11.5	± 0.5	13	11.9	± 0.4	21	7.79	± 0.50
39	Y	2.09	± 0.03	8	1.64	± 0.04	12	1.80	± 0.03	20	1.50	± 0.10
40	Zr	3.90	± 0.07	5	4.15	± 0.50	10	4.08	± 0.36	15	3.79	± 0.28
41	Nb	0.386	± 0.006	5	0.353	± 0.004	8	0.369	± 0.004	13	0.279	± 0.015
42	Mo	0.987	± 0.014	5	1.05	± 0.01	8	1.02	± 0.01	13	0.976	± 0.050
44	Ru	0.551	± 0.030	3	0.643	± 0.018	4	0.625	± 0.016	7	0.666	± 0.040
45	Rh				0.150	± 0.010	1	0.150	± 0.010	1	0.133	± 0.008
46	Pd	0.503	± 0.010	3	0.804	± 0.009	4	0.744	± 0.007	7	0.558	± 0.030
47	Ag	0.195	± 0.009	1	0.195	± 0.006	2	0.195	± 0.005	3	0.204	± 0.008
48	Cd	0.706	± 0.023	8	0.754	± 0.017	12	0.737	± 0.014	20	0.679	± 0.024
49	In	0.103	± 0.004	3	0.0912	± 0.0027	4	0.0976	± 0.0023	7	0.0786	± 0.0040
50	Sn	1.31	± 0.03	4	1.98	± 0.13	8	1.85	± 0.11	12	1.63	± 0.16
51	Sb	0.155	± 0.007	5	0.174	± 0.006	8	0.166	± 0.005	13	0.169	± 0.018
52	Te	2.19	± 0.05	3	2.39	± 0.15	4	2.35	± 0.12	7	2.31	± 0.18
53	I										0.770	± 0.620
54	Xe	0.000560	± 0.000004	14	0.000616	± 0.000009	6	0.000572	± 0.000004	20	0.000174	± 0.0000000
55	Cs	0.212	± 0.003	8	0.199	± 0.004	11	0.205	± 0.002	19	0.188	± 0.012
56	Ba	3.38	± 0.06	8	2.87	± 0.05	13	3.02	± 0.04	21	2.39	± 0.16
57	La	0.303	± 0.004	8	0.275	± 0.003	11	0.288	± 0.002	19	0.244	± 0.016
58	Ce	0.785	± 0.010	8	0.654	± 0.017	12	0.702	± 0.011	20	0.627	± 0.052
59	Pr	0.124	± 0.002	8	0.109	± 0.002	11	0.116	± 0.001	19	0.0951	± 0.0066
60	Nd	0.666	± 0.013	8	0.536	± 0.024	12	0.583	± 0.016	20	0.472	± 0.036
62	Sm	0.208	± 0.004	8	0.181	± 0.005	11	0.194	± 0.003	19	0.153	± 0.012
63	Eu	0.0818	± 0.0011	8	0.0683	± 0.0012	11	0.0748	± 0.0008	19	0.0577	± 0.0050
64	Gd	0.303	± 0.005	8	0.246	± 0.004	11	0.273	± 0.003	19	0.208	± 0.018
65	Tb	0.0541	± 0.0007	8	0.0451	± 0.0006	11	0.0494	± 0.0005	19	0.0380	± 0.0030
66	Dy	0.375	± 0.004	8	0.313	± 0.004	11	0.343	± 0.003	19	0.252	± 0.020
67	Ho	0.0823	± 0.0011	8	0.0676	± 0.0006	11	0.0747	± 0.0006	19	0.0563	± 0.0044
68	Er	0.247	± 0.004	8	0.206	± 0.003	11	0.226	± 0.002	19	0.164	± 0.012
69	Tm	0.0381	± 0.0006	8	0.0315	± 0.0006	11	0.0347	± 0.0004	19	0.0259	± 0.0024
70	Yb	0.247	± 0.003	8	0.205	± 0.003	11	0.225	± 0.002	19	0.167	± 0.014
71	Lu	0.0368	± 0.0009	8	0.0313	± 0.0006	11	0.0340	± 0.0005	19	0.0249	± 0.0020
72	Hf	0.120	± 0.003	5	0.123	± 0.007	8	0.122	± 0.004	13	0.106	± 0.008
73	Ta	0.0460	± 0.0009	5	0.469	± 0.007	8	0.268	± 0.004	13	0.0148	± 0.0014
74	W	0.106	± 0.004	5	0.141	± 0.003	8	0.124	± 0.002	13	0.102	± 0.014
75	Re	0.0364	± 0.0019	3	0.0463	± 0.0024	3	0.0413	± 0.0015	6	0.0369	± 0.0028
76	Os	0.460	± 0.019	4	0.494	± 0.011	4	0.476	± 0.011	8	0.475	± 0.020
77	Ir	0.448	± 0.008	4	0.542	± 0.011	4	0.492	± 0.007	8	0.474	± 0.020
78	Pt	0.767	± 0.021	3	0.891	± 0.025	3	0.828	± 0.017	6	0.931	± 0.072
79	Au	0.193	± 0.002	1	0.0737	± 0.0016	1	0.159	± 0.002	2	0.147	± 0.024
80	Hg										0.288	± 0.140
81	Tl	0.117	± 0.004	8	0.119	± 0.005	11	0.118	± 0.003	19	0.141	± 0.014
82	Pb	2.75	± 0.07	8	2.93	± 0.06	11	2.84	± 0.05	19	2.64	± 0.16
83	Bi	0.109	± 0.003	8	0.111	± 0.004	11	0.110	± 0.002	19	0.113	± 0.016
90	Th	0.0332	± 0.0011	8	0.0336	± 0.0009	11	0.0334	± 0.0007	19	0.0298	± 0.0030
92	U	0.00924	± 0.00034	8	0.00922	± 0.00048	11	0.00923	± 0.00030	19	0.00816	± 0.00106

documented dispersion of literature values for CIs, whereas the calculated $^{54}\text{Cr}/^{52}\text{Cr}$ ratio of a total of ~ 90 mg of the bulk Ryugu sample is consistent with the CI value (Yokoyama *et al.*, 2023b). This observation suggests the presence of mm-scale $^{54}\text{Cr}/^{52}\text{Cr}$ variability in the bulk Ryugu samples, which could have primarily been caused by fluid-driven parent body aqueous alteration. On the other hand, Ryugu showed greater s-process depletion of Mo isotopes compared to any known bulk CCs, including CIs (Nakanishi *et al.*, 2023). The different Mo isotopic compositions of Ryugu and CIs could be caused by biased sampling of Ryugu materials. Ryugu is enriched in aqueously formed secondary minerals with s-process-poor Mo isotopes, resulting from the physicochemical separation of s-process-rich presolar grains and a complementary s-process-poor aqueous fluid in the Ryugu parent body. However, incomplete digestion of s-process-rich presolar SiC during dissolution of Ryugu samples in the laboratory cannot be ruled out. The small-scale isotopic heterogeneity of Ryugu, as suggested by the two case studies on Cr and Mo isotopes, is most likely related to the variability of elemental abundances in Ryugu samples due to the heterogeneous distribution of secondary minerals, as discussed below.

3. Evaluation of Ryugu sample heterogeneity

3.1. Variation of elemental abundances in Ryugu samples

Figure 2 shows the CI-normalized abundances of 18 selected elements in the Ryugu samples (Ito *et al.*, 2022; Nakamura *et al.*, 2022; Yokoyama *et al.*, 2023a). The diamond data points are data measured by XRF in Yokoyama *et al.* (2023a) using C0108 (24 mg), and the circle symbols are those obtained by ICP-MS measurements in the same study using A0106 and A0107 combined (24 mg) and C0108 (pre-measured by XRF). The ICP-MS results obtained from the two samples are generally in good agreement, with the maximum relative percentage difference ($\text{RPD} = |X_{\text{A0106+A0107}} - X_{\text{C0108}}| / (X_{\text{A0106+A0107}}/2 + X_{\text{C0108}}/2) \times 100$) of 22% for P. The boxplots in Fig. 2a show the variation of analytical data for 0.18–3.3 mg of Ryugu samples ($n = 19$: Ito *et al.*, 2022; Nakamura *et al.*, 2022), which show large dispersions for some elements, including P ($0.2\text{--}2.1 \times \text{CI}$), Ca ($0.6\text{--}2.8 \times \text{CI}$), Mn ($0.5\text{--}2.3 \times \text{CI}$), Sr ($0.6\text{--}2.8 \times \text{CI}$), La ($0.4\text{--}1.5 \times \text{CI}$), Gd ($0.3\text{--}2.2 \times \text{CI}$), and Yb ($0.1\text{--}2.4 \times \text{CI}$)

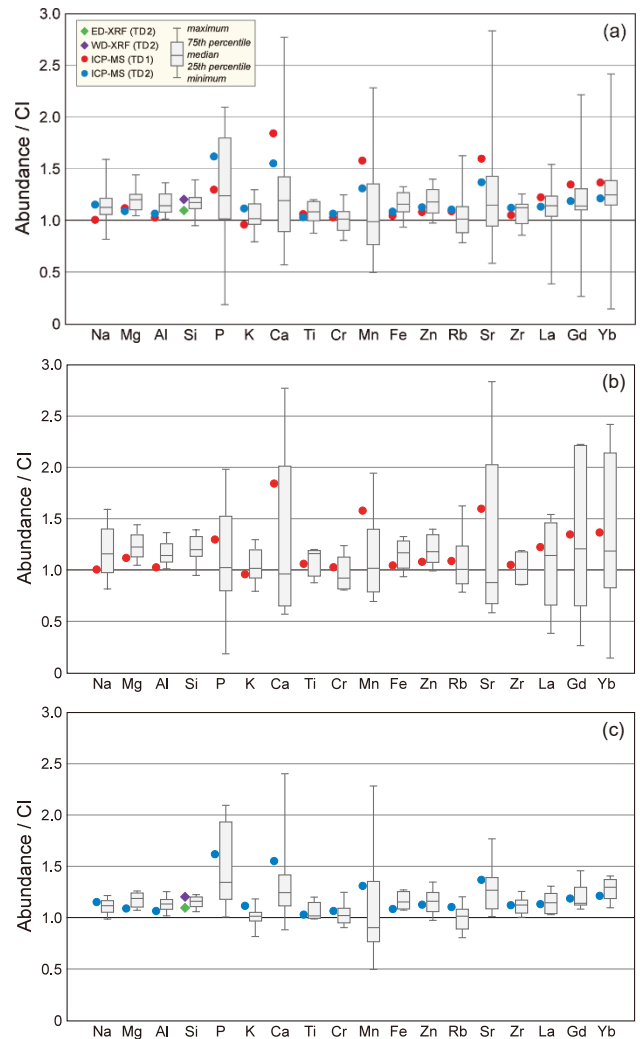


Fig. 2 CI-normalized elemental abundances in bulk Ryugu samples from (a) Chambers A (“TD1”) and C (“TD2”) combined, (b) Chamber A, and (c) Chamber C. The diamonds (XRF) and circles (ICP-MS) represent data obtained from the measurements of ~ 25 mg powdered Ryugu samples (Yokoyama *et al.*, 2023a). Boxplots were produced from the ICP-MS data of 16 individual Ryugu grains with digested masses of 0.2–3 mg, except for Si, which was measured by electron probe (Nakamura *et al.*, 2022).

compared with the other elements that show dispersions mostly in the range of $0.8\text{--}1.4 \times \text{CI}$. Specifically, samples from Chamber A ($n = 8$) show larger dispersions in these elements than samples from Chamber C ($n = 11$) (Figs. 2b, 2c).

The observed variations in some elements for the measurements of relatively small samples (< 3.3 mg) most likely stems from the presence of aqueously formed secondary minerals in Ryugu (e.g., carbonates and phosphates), in which some specific elements, including P, Mn, Sr, and rare earth elements (REEs), are strongly partitioned when these minerals precipitate.

The modal abundances of carbonates (0.43–6.93%) and phosphates (0.16–1.88%) vary from fragment to fragment in Ryugu (Nakamura *et al.*, 2022), such that the obtained elemental abundances for small-size samples are controlled by the amount of relevant minerals involved (i.e., nugget effect). Similar variability can be observed for the abundances of P and Ca in fragments of CI chondrites, resulting from the different mineralogical compositions of the measured fragments (Morlok *et al.*, 2006). Even in the largest 24 mg Ryugu sample, the influence of carbonates and phosphates can be seen for P, Ca, and Mn (Fig. 2), as the two bulk samples (TD1 and TD2) showed ~20% of RPD in the abundances of these elements. Therefore, the estimation of the Solar System composition using currently all available Ryugu elemental abundances is challenging due to the nugget effect of carbonates and phosphates, and possibly other accessory minerals such as oxides and sulfides.

3.2. Nugget effect of secondary minerals

There are several telltale characteristics of the nugget effect of secondary minerals. In particular, "bulk" analyses of relatively small samples should define mixing curves between the "true bulk" and the mineral composition in elemental ratio plots (Fig. 3). Evaluating the extent of variation for elemental ratios is specifically important when the ratio is a combination of two elements containing a radioactive isotope and its daughter nuclide. In this case, the variation of the elemental ratio is reflected in the variation of the isotopic ratios of the daughter nuclide as a function of time (i.e., chronometer). As mentioned above, small Ryugu samples show large dispersions for Mn ($0.5\text{--}2.3 \times \text{CI}$) and Sr ($0.6\text{--}2.8 \times \text{CI}$). Thus, key elemental ratios to be discussed here include Mn/Cr and Rb/Sr, which represent the parent/daughter isotopic ratio for the $^{53}\text{Mn}\text{--}^{53}\text{Cr}$ and $^{87}\text{Rb}\text{--}^{87}\text{Sr}$ chronometers. Note that detailed determination of the bulk Mn/Cr and Rb/Sr ratios for Ryugu, as well as the $^{53}\text{Cr}/^{52}\text{Cr}$ and $^{87}\text{Sr}/^{86}\text{Sr}$ ratios, is important for discussing the chondritic evolution of radiogenic isotopes, which in turn can help determining the timing of volatile losses for various planetary bodies in the early Solar System (e.g., Hans *et al.*, 2013). To this end, we evaluate the influence of three mineral phases, carbonate (dolomite; $\text{CaMg}(\text{CO}_3)_2$), phosphate (apatite; $\text{Ca}_5(\text{PO}_4)_3(\text{OH},\text{F},\text{Cl})$), and oxide (magnetite; Fe_3O_4), on the variation of elemental abundance ratios in Ryugu samples measured in previous studies. Other carbonates and phosphates (e.g., breunnerite; $(\text{Mg}, \text{Fe})\text{CO}_3$, calcite; CaCO_3 , and Na-Mg phosphate) found in Ryugu samples

are less abundant compared to the abovementioned minerals, and they are not considered here. Additionally, sulfides are not taken into the calculation since they would not play a significant role in changing the Mn/Cr and Rb/Sr ratios in bulk Ryugu. The elemental abundances of dolomite, apatite, and magnetite, taken from Bazi *et al.* (2022) and Nakamura *et al.* (2022) used in the following discussion are summarized in Table 2.

As mentioned in the previous section, individual Ryugu samples contain varying amounts of dolomite, which has higher Mn/Cr and lower Fe/Mn ratios than the bulk CI chondrite. Consequently, these ratios are well correlated in Ryugu samples (Fig. 3a), and the observed variation can be generally explained by the admixture (up to 5.6 wt.%) or removal (up to 2.3 wt.%) of dolomite to or from the bulk CI chondrite (Lodders, 2021). Of note, the bulk Ryugu sample reconstructed from all measured data (filled star) is distinct from the CI chondrite (open star), indicating an approximately 1% enrichment of dolomite relative to the CI chondrite. Apatite in Ryugu is also expected to have higher Mn/Cr and lower Fe/Mn ratios than the bulk CI chondrite, and the addition or removal of apatite relative to or from CI results in a mixing relationship similar to that observed for CI-dolomite mixing. Nevertheless, the impact of apatite on Mn/Cr and Fe/Mn ratios is not as pronounced as that of dolomite at a given modal abundance, due to the relatively low Mn abundance in apatite (Table 2). Unlike dolomite and apatite, magnetite is extremely enriched in Fe but depleted in Mn, and has a Mn/Cr ratio lower than bulk CI. Thus, the addition or removal of magnetite relative to or from CI shows a distinct trajectory in Fig. 3a, which can explain the data points of those Ryugu grains that slightly deviate from the mixing relationship between CI and dolomite/apatite.

Dolomite has a lower Rb/Sr ratio than CI (Table 2) since Sr^{2+} can easily substitute the Ca^{2+} site in the dolomite crystal. A weak positive trend of the Ryugu data in the $(\text{Rb}/\text{Sr})_{\text{N}}$ versus $(\text{Fe}/\text{Mn})_{\text{N}}$ plot thus indicates admixture or removal of dolomite relative to bulk CI chondrite (Fig. 3b), although the deviation of individual data points from the CI-dolomite mixing curve is more conspicuous compared to the Mn/Cr-Fe/Mn correlation (Fig. 3a). Apatite, which also has a Ca^{2+} site as a major constituent, plays a significant role in varying the Rb/Sr ratio of the Ryugu samples without affecting the Fe/Mn ratio. For this reason, the addition or removal of apatite to or from CI chondrite results in an almost vertical trend in Fig. 3b. As opposed to this correlation, the admixture of magnetite alone slightly affects the Fe/Mn

Table 2 Elemental abundances of secondary minerals

Element	Dolomite		Magnetite		Apatite	
	$\mu\text{g/g}$	References	$\mu\text{g/g}$	References	$\mu\text{g/g}$	References
P	0	B22	0	B22	163200	B22
Ti	350	B22	3633	B22	0	B22
Cr	2047	B22	2367	B22	1500	B22
Mn	49100	B22	508	B22	7300	B22
Fe	20300	B22	723600	B22	21100	B22
Rb	0	M84	0	#1	0	#1
Sr	97.8	B22, N22	0	B22	522	B22, N22

References: B22 (Bazi *et al.*, 2022); M84 (Macdougall *et al.*, 1984), N22 (Nakamura *et al.*, 2022).

#1: The abundance of Rb is assumed to be zero, since Rb is almost completely excluded from the mineral structure.

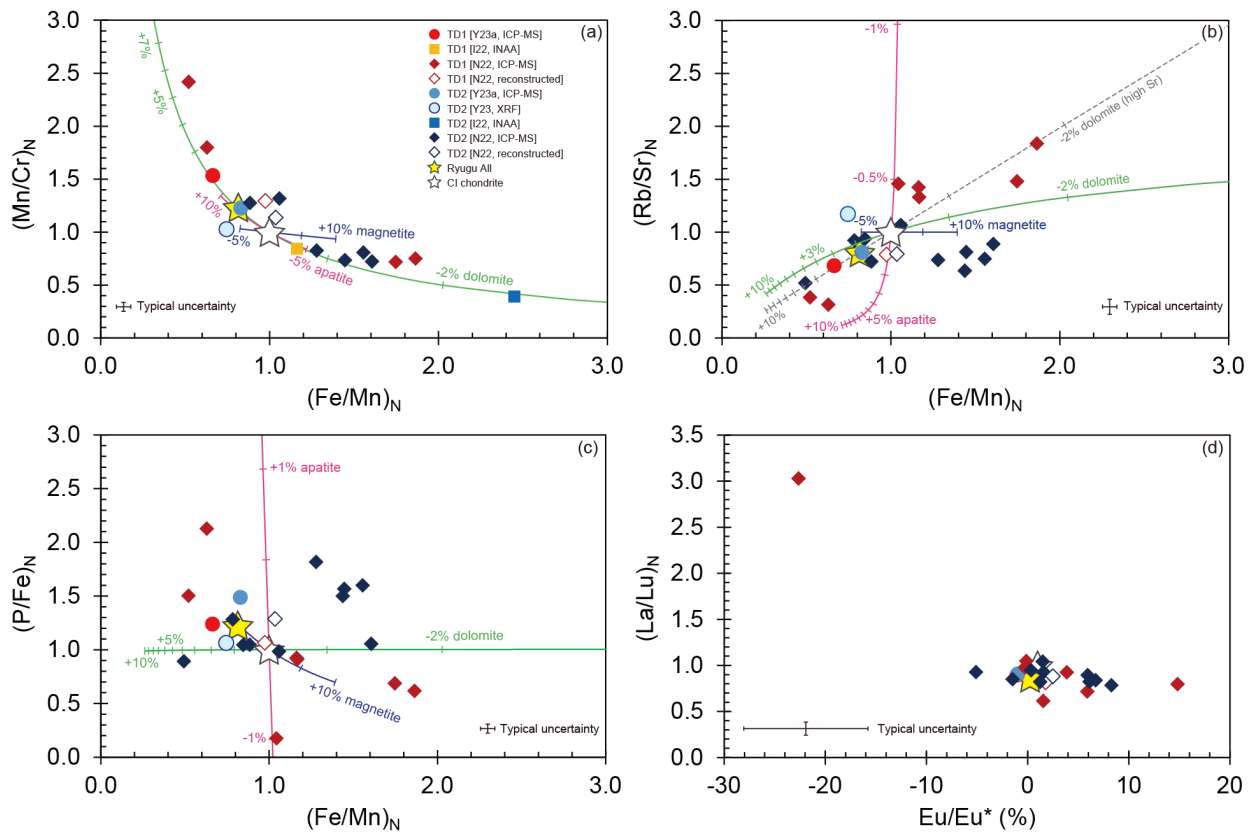


Fig. 3 Correlations between CI chondrite-normalized ratios of (a) Mn/Cr–Fe/Mn, (b) Rb/Sr–Fe/Mn, and (c) P/Fe–Fe/Mn for bulk Ryugu samples obtained by Yokoyama *et al.* (2023a) (“Y23a”), Nakamura *et al.* (2022) (“N22”), and so on I22 (Ito *et al.*, 2022). Open stars are CI composition (Lodders, 2021) and yellow stars are average Ryugu composition (Table 1). The curves represent the addition or removal of dolomite (green), magnetite (blue), and apatite (pink) relative to the bulk CI chondrite. (d) Diagram between CI-normalized La/Lu ratio and Eu anomaly (see text for definition). The crosses are typical measurement uncertainties for ICP-MS analysis (3% for P, Mn, Cr, and Fe, and 5% for the other elements) for the value 1 (all elemental ratios) and for the value 0% (Eu/Eu*).

ratio, so the role of magnetite is not significant in producing the observed variation in this figure. Interestingly, the Rb/Sr ratio of Chamber A samples covaries with the Fe/Mn ratio, whereas that of Chamber C samples remains relatively uniform regardless of the Fe/Mn ratio. This observation may indicate that dolomite in

Chamber A samples coprecipitated with apatite during aqueous alteration, as suggested by a negative correlation between (P/Fe)_N and (Fe/Mn)_N values for Chamber A samples, except for one with an extremely low P/Fe ratio (Fig. 3c). It is noteworthy, however, that such a correlated behavior between apatite and dolomite, as

well as any other combination of secondary minerals, is not seen in the mineral modal abundances of the samples measured by Nakamura *et al.* (2022) (Fig. 4). Thus, the observed positive correlation between Rb/Sr and Fe/Mn ratios for the Chamber A samples may reflect another phenomenon. One possibility is that the dolomite in the Chamber A samples has a Sr mass fraction twice (~200 ppm) that estimated in previous studies, making the CI-dolomite mixing line much steeper (dashed line in Fig. 3c). In this case, the Chamber C samples with relatively high Fe/Mn ratios deviate more from the CI-dolomite mixing line, requiring the involvement of apatite to lower the Rb/Sr ratio for these samples.

Overall, carbonates appear to be the most important mineral whose modal abundance largely controls the Mn/Cr and Rb/Sr ratios in individual Ryugu samples. The nugget effect of phosphate grains is also significant, affecting the Rb/Sr ratio of some Ryugu samples. In carbonaceous and ordinary chondrites, a nugget effect associated with the presence of phosphates has been identified for REEs (Dauphas and Pourmand, 2015). Since phosphates in ordinary chondrites have high La/Lu ratios and negative Eu/Eu* anomalies ($\text{Eu}/\text{Eu}^* = \text{Eu}_N/(\text{Sm}_N^{0.45} \times \text{Gd}_N^{0.55})$), the presence of phosphate nuggets in ordinary chondrites resulted in a negative correlation between the La/Lu ratio and the Eu/Eu* value (Dauphas and Pourmand, 2015). In contrast, phosphates in Ryugu lack these properties and are more difficult to detect (Nakamura *et al.*, 2022). Indeed, one sample (A0085) shows an exceptionally high La/Lu ratio with a large negative Eu/Eu* anomaly (Fig. 3d), whereas the $(\text{P}/\text{Fe})_N$ value (= 0.18) and the modal abundance of phosphates (= 0.25%) of this sample are both extremely low compared to the other Ryugu samples (Figs. 3c, 4). Thus, the abundance of REEs in Ryugu could be largely controlled by the presence of other minor phase(s).

3.3. Statistical analysis of the nugget effect

Another telltale signature of a nugget effect is that the dispersion in elemental ratios should decrease as the inverse of the square root of the mass of the homogenized sample (Dauphas and Pourmand, 2015). Such mass-dependent dispersion in elemental ratios is consistent with a sampling problem associated with the nugget effect. Considering two elements with mass fractions C_1 and C_2 in a sample of mass = m , the dispersion of the elemental ratio $R = C_2/C_1$ can be calculated by the following equation (Dauphas and Pourmand, 2015);

$$\sigma_R \approx \frac{r(\rho_{\text{nugget}}/\rho_{\text{matrix}})}{[1 + rf(\rho_{\text{nugget}}/\rho_{\text{matrix}})]^2} \sqrt{\frac{f\rho_{\text{matrix}}\pi d^3}{6m}} \times |R_{\text{nugget}} - R_{\text{matrix}}| \quad (3)$$

where r is $C_{1_nugget}/C_{1_matrix}$, ρ is the density, f is the volume fraction of nuggets, and d is the particle diameter of the nugget. Figure 5 shows the Mn/Cr and Rb/Sr ratios of individual Ryugu samples measured in previous studies, plotted against the digested mass. The

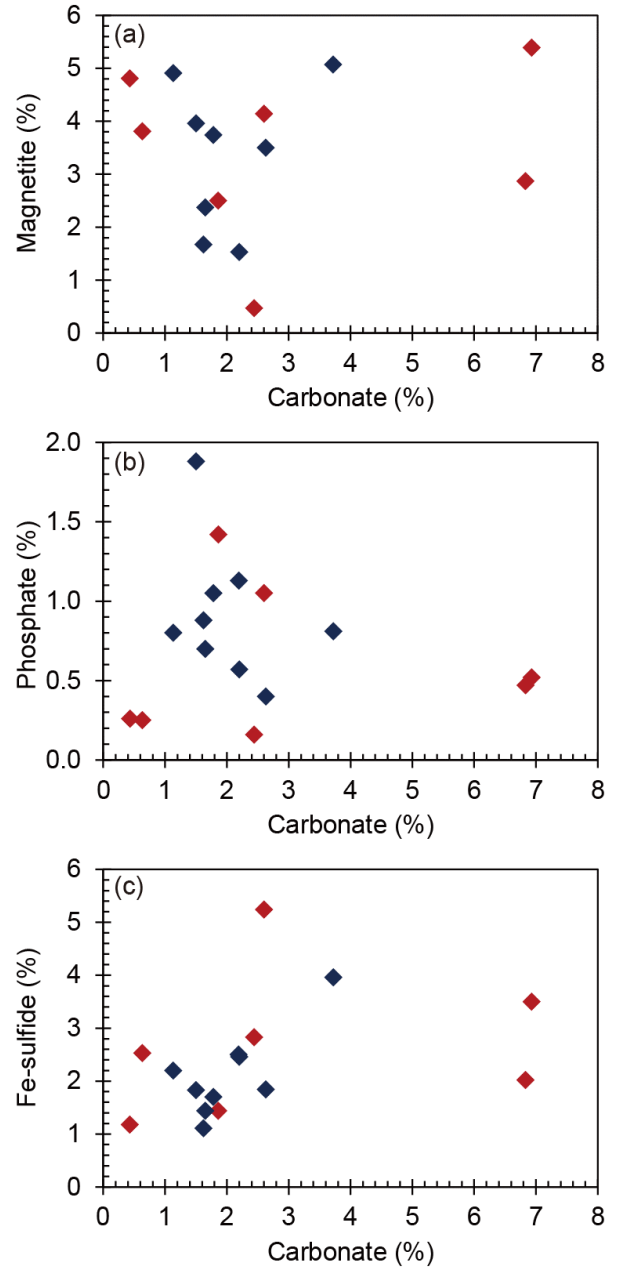


Fig. 4 The modal abundances of carbonate and (a) magnetite, (b) phosphate, and (c) Fe-sulfide in Ryugu fragments measured by Nakamura *et al.* (2022) show no correlations. The red and blue diamonds are samples from Chamber A (TD#1) and C (TD#2), respectively.

curves in this figure show the estimated dispersion ($\pm 2\sigma$) of the Mn/Cr and Rb/Sr ratios calculated from equation (3) as a function of the sample mass used, assuming carbonates as the nugget phase. The elemental abundances in carbonates and matrix (i.e., non-carbonate phase) are given in [Tables 1](#) and [2](#). The other parameters used in the calculation are: $\rho_{\text{nugget}} = 2.84 \text{ g/cm}^3$, $\rho_{\text{matrix}} = 2.587 \text{ g/cm}^3$ (grain density: Nakamura *et al.*, 2022), $f = 0.025$ (Nakamura *et al.*, 2022), and $d = 0.10 \text{ mm}$.

As shown in [Fig. 5](#), the dispersions of the Mn/Cr and Rb/Sr ratios for the individual Ryugu data are significantly larger than the dispersion estimated from equation (3) (thin red curves). This inconsistency is caused by an inappropriate assumption of the parameters used in the calculation and/or the presence of additional nugget phases other than carbonates (e.g., phosphates). In particular, increasing the d and f values of carbonates in equation (3) monotonically increases the σ_R value; changing the d value from 0.10 to 0.16 mm makes the σ_R value twice as high, although such a large carbonate grain rarely exists in Ryugu (Nakamura *et al.*, 2022). Thus, the observed inconsistency suggests a non-uniform distribution of various nugget minerals of different sizes (d) at the mm-scale of the Ryugu fragments examined in the elemental abundance measurements by Nakamura *et al.* (2022) and Ito *et al.* (2022).

To overcome this difficulty, we instead calculated the dispersion for the smaller fragments and calculated the predicted dispersion for larger masses. Having determined that unrepresentative sampling of carbonates is likely responsible for the dispersion in certain elemental ratios, we can predict the expected dispersion when large sample masses are digested as follows;

$$\sigma_R(M) = \sigma_R(\bar{m}) \sqrt{\bar{m}/M} \quad (4)$$

where M is the expected sample mass to be digested, \bar{m} is the average mass of the digested smaller fragments, and $\sigma_R(\bar{m})$ is the standard deviation of R for the measurement of the smaller fragments. Here, \bar{m} and $\sigma_R(\bar{m})$ are determined using the data obtained in the measurements of smaller fragments ($< 3.3 \text{ mg}$) by Nakamura *et al.* (2022) and Ito *et al.* (2022). The following equation then gives the possible range of R in a Ryugu analysis digesting a homogenized sample of mass M ;

$$R(M) = \bar{R} \pm 2\sigma_R(M) \quad (5)$$

where \bar{R} is the estimated Mn/Cr or Rb/Sr ratio of the bulk Ryugu of mass M ([Table 1](#)).

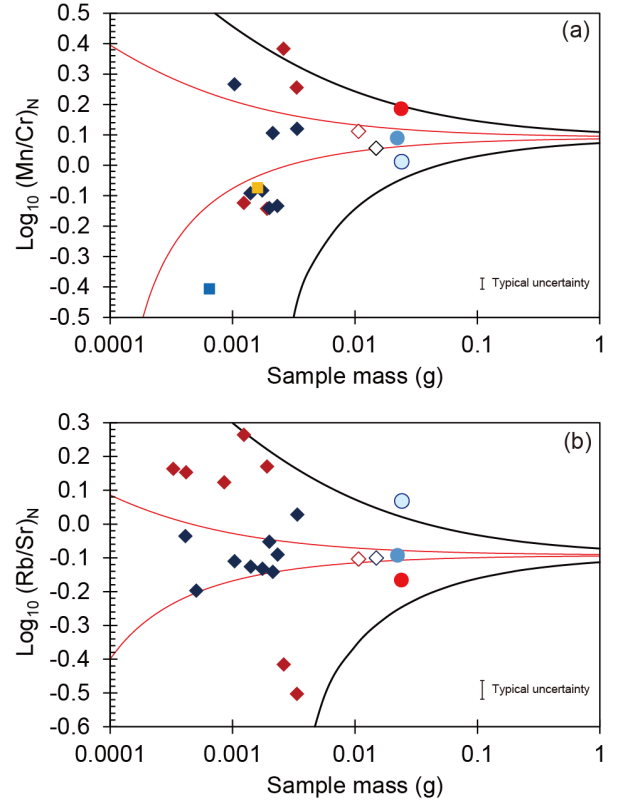


Fig. 5 Elemental ratios of (a) Mn/Cr and (b) Rb/Sr, both of which are sensitive to carbonate nugget effects, plotted against sample mass. Symbols are the same as in [Fig. 3](#). In the presence of a nugget effect, the dispersion of elemental ratios is expected to decrease as the inverse of the square root of the mass of the homogenized/digested sample (red thin curves) (Dauphas and Pourmand, 2015). However, this theoretical prediction underestimates the actual dispersion of the Ryugu data, due to non-uniform distribution of nugget minerals of different sizes within the mm-scale of the Ryugu fragments. The bold black curves are the estimated data dispersion calculated using the dispersion of data obtained from smaller Ryugu fragments ($< 3.3 \text{ mg}$, see main text for references). The vertical bars are typical measurement uncertainties for ICP-MS analysis (3% for Mn and Cr and 5% for Rb and Sr).

The bold black curves in [Fig. 5](#), calculated from equation (5), show the dispersion (2σ) of the Mn/Cr and Rb/Sr ratios for a Ryugu measurement assuming a sample mass M . It should be noted that the calculated dispersion corresponds to the maximum range of difference in the Mn/Cr and Rb/Sr ratios of the measured sample (mass = M) from those of the “true” bulk Ryugu sample, and thus represents the “analytical error” of these ratios. When the homogenized Ryugu sample weighs 0.1 g, the expected errors for the Mn/Cr and Rb/Sr ratios are $\pm 13\%$ and $\pm 15\%$, respectively. This level of analytical error is much larger than the

measurement uncertainties of elemental ratios determined by a common ICP-MS instrument, which are better than $\pm 3\%$ and $\pm 1\%$ for the calibration curve and isotope dilution methods, respectively. Homogenization of more samples reduces the expected error of elemental ratios. To achieve within $\pm 5\%$ error, the required amount of Ryugu sample to be homogenized is 0.7 g and 0.85 g for Mn/Cr and Rb/Sr ratios, respectively. To further improve the analytical error better than $\pm 3\%$, > 2 g of homogenized Ryugu sample is required.

It should be noted that the uncertainties of the Mn/Cr and Rb/Sr ratios are $\pm 11\%$ and $\pm 10\%$ for CI chondrites (2σ), and $\pm 24\%$ and $\pm 46\%$ for the Sun (3D model for outer convection zone), respectively (Lodders, 2021). Given the measurement uncertainties for ICP-MS, elemental ratio analysis of the homogenized Ryugu sample within $\pm 5\%$ error is an achievable goal. Our statistical analysis shows that much of the variation in chemical composition between Ryugu grains is due to non-representative sampling of mineral phases highly enriched in some elements, which can be reduced sufficiently by measuring a homogeneous powder prepared from a relatively large sample mass (~ 1 g).

4. Future prospects of Ryugu sample analysis

The scatter of the chemical composition in published Ryugu data (Fig. 2) is likely caused by a nugget effect of secondary minerals, most likely carbonates and phosphates. As discussed in the previous section, this nugget effect can be mitigated by measuring homogenized material prepared from a relatively large sample mass. Here, we suggest establishing a new consortium to determine the representative chemical compositions of Ryugu by measuring aliquots from a large homogenized sample. The ultimate goal of such a consortium is to provide a new international reference for the chemical composition of the Solar System based on the elemental abundances (and isotopic compositions) of Ryugu and CI chondrites and the composition of the solar photosphere. The new reference values will serve as an important benchmark for the Solar System composition in a variety of scientific fields.

To fulfill the purpose of the consortium, we recommend using ~ 1 g (minimum 0.85 g) of stored Ryugu samples. As discussed above, such an amount of homogeneous powder will suppress the dispersion of elemental ratios (e.g., Mn/Cr, Rb/Sr) to $\pm 5\%$ or less. The stored Ryugu samples suitable for the preparation of the

powdered Ryugu would be an aggregate of many sub-millimeter grains from each Chambers A and C. Combining samples from different chambers should be avoided because the samples in Chambers A and C were collected from two different touch-down sites on the Ryugu body, the former representing surface materials and the latter probably containing mostly subsurface materials derived from the artificial crater. Thus, mixing samples from the two chambers will hinder the opportunity to investigate the chemical/isotopic heterogeneity present in the Ryugu samples from distinct locations, which is key to understanding the evolutionary history of the Ryugu parent body including aqueous alteration.

The newly obtained more precise chemical composition of Ryugu will be used by multidisciplinary communities in various scientific fields including astronomy, astrobiology, cosmochemistry, geochemistry, geology, and planetary physics. For instance, a comparison of elemental abundances between CI chondrites, Ryugu, and new asteroidal materials collected from B-type asteroid (101955) Bennu by the OSIRIS-REx mission (Lauretta *et al.*, 2017) will expand our knowledge regarding the formation of primordial small bodies in the early Solar System, as well as the chemical heterogeneity of the solar nebula. Comparative studies of the chemical compositions of chondrites, Ryugu, and the terrestrial mantle will facilitate the discussion on the origin of Earth and rocky planets, including the origin of Earth's water. More importantly, the new Ryugu data, coupled with the elemental abundances of the solar photosphere, will serve as an important reference of the Solar System composition for understanding elemental abundances in other astronomical objects such as stars and the interstellar medium, as well as for providing a fundamental anchor point at 4.5 Ga for evaluating various Galactic Chemical Evolution models. The data would be beneficial for updating the astrophysical database including the Atomic Data for Astrophysics (ATOMDB: <http://www.atomdb.org/>), which allows accurate modeling of the emission and absorption spectra of various astrophysical objects, including supernova remnants, galaxy clusters, and active galactic nuclei.

Acknowledgments We thank H. Yurimoto and all the members of the Hayabusa2 Initial Analysis Chemistry Team and the Initial Analysis Core. Discussion with team members of the Hayabusa2 Sample Allocation Committee (HSAC) has dramatically improved the quality of this paper. This research was supported by JSPS KAKENHI Grants to TY (23H00143, 21KK0058, and 20H04609).

References

- Amelin, Y., Krot, A. N., Hutcheon, I. D. and Ulyanov, A. A. (2002) Lead isotopic ages of chondrules and calcium-aluminum-rich inclusions. *Science*. **297**, 1678-1683.
- Bazi, B., Tack, P., Lindner, M., Vekemans, B., De Pauw, E., Tkalcec, B., Brenker, F. E., Garrevoet, J., Falkenberg, G. and Yabuta, H. (2022) Trace-element analysis of mineral grains in Ryugu rock fragment sections by synchrotron-based confocal X-ray fluorescence. *Earth, Planets and Space*. **74**, 161.
- Bizzarro, M., Schiller, M., Yokoyama, T., Abe, Y., Aléon, J., Alexander, C. M. O'D., Amari, S., Amelin, Y., Bajo, K.-i. and Bouvier, A. (2023) The Magnesium Isotope Composition of Samples Returned from Asteroid Ryugu. *Astrophys. J.* **958**, L25.
- Connelly, J. N., Bizzarro, M., Krot, A. N., Nordlund, A., Wielandt, D. and Ivanova, M. A. (2012) The absolute chronology and thermal processing of solids in the solar protoplanetary disk. *Science*. **338**, 651-655.
- Dauphas, N. and Pourmand, A. (2015) Thulium anomalies and rare earth element patterns in meteorites and Earth: Nebular fractionation and the nugget effect. *Geochim. Cosmochim. Acta*. **163**, 234-261.
- Hans, U., Kleine, T. and Bourdon, B. (2013) Rb–Sr chronology of volatile depletion in differentiated protoplanets: BABI, ADOR and ALL revisited. *Earth Planet. Sci. Lett.* **374**, 204-214.
- Hopp, T., Dauphas, N., Abe, Y. *et al.* (2022) Ryugu's nucleosynthetic heritage from the outskirts of the Solar System. *Science Advances*. **8**, eadd8141.
- Hu, Y., Moynier, F., Dai, W. *et al.* (2024) Pervasive aqueous alteration in the early Solar System revealed by potassium isotopic variations in Ryugu samples and carbonaceous chondrites. *Icarus*. **409**, 115884.
- Ito, M., Tomioka, N., Uesugi, M. *et al.* (2022) A pristine record of outer Solar System materials from asteroid Ryugu's returned sample. *Nature Astronomy*.
- Jochum, K. P., Weis, U., Schwager, B., Stoll, B., Wilson, S. A., Haug, G. H., Andreae, M. O. and Enzweiler, J. (2016) Reference Values Following ISO Guidelines for Frequently Requested Rock Reference Materials. *Geostandard. Geoanalytic. Res.* **40**, 333-350.
- Kawasaki, N., Nagashima, K., Sakamoto, N., Matsumoto, T., Bajo, K.-i., Wada, S., Igami, Y., Miyake, A., Noguchi, T. and Yamamoto, D. (2022) Oxygen isotopes of anhydrous primary minerals show kinship between asteroid Ryugu and comet 81P/Wild2. *Science Advances*. **8**, eade2067.
- Lauretta, D., Balram-Knutson, S., Beshore, E., Boynton, W., Drouet d'Aubigny, C., DellaGiustina, D., Enos, H., Golish, D., Hergenrother, C. and Howell, E. (2017) OSIRIS-REx: sample return from asteroid (101955) Bennu. *Space Sci. Rev.* **212**, 925-984.
- Lodders, K. (2020) Solar elemental abundances. *Oxford Research Encyclopedia of Planetary Science*.
- Lodders, K. (2021) Relative atomic solar system abundances, mass fractions, and atomic masses of the elements and their isotopes, composition of the solar photosphere, and compositions of the major chondritic meteorite groups. *Space Sci. Rev.* **217**, 1-33.
- Maccougall, J., Lugmair, G. and Kerridge, J. (1984) Early solar system aqueous activity: Sr isotope evidence from the Orgueil CI meteorite. *Nature*. **307**, 249-251.
- Morlok, A., Bischoff, A., Stephan, T., Floss, C., Zinner, E. and Jessberger, E. K. (2006) Brecciation and chemical heterogeneities of CI chondrites. *Geochim. Cosmochim. Acta*. **70**, 5371-5394.
- Moynier, F., Dai, W., Yokoyama, T. *et al.* (2022) The Solar System calcium isotopic composition inferred from Ryugu samples. *Geochemical Perspectives Letters*. **24**.
- Nakamura, E., Kobayashi, K., Tanaka, R. *et al.* (2022) On the origin and evolution of the asteroid Ryugu: A comprehensive geochemical perspective. *Proceedings of the Japan Academy, Series B*. **98**, 227-282.
- Nakamura, T., Matsumoto, M., Amano, K. *et al.* (2023) Formation and evolution of carbonaceous asteroid Ryugu: Direct evidence from returned samples. *Science*. **379**, eabn8671.
- Nakanishi, N., Yokoyama, T., Ishikawa, A. *et al.* (2023) Nucleosynthetic s-Process Depletion in Mo from Ryugu samples returned by Hayabusa2. *Geochemical Perspectives Letters*. **28**, 31-36.
- Naraoka, H., Takano, Y., Dworkin, J. P. *et al.* (2023) Soluble organic molecules in samples of the carbonaceous asteroid (162173) Ryugu. *Science*. **379**, eabn9033.
- Oba, Y., Koga, T., Takano, Y., Ogawa, N. O., Ohkouchi, N., Sasaki, K., Sato, H., Glavin, D. P., Dworkin, J. P., Naraoka, H., Tachibana, S., Yurimoto, H., Nakamura, T., Noguchi, T., Okazaki, R., Yabuta, H., Sakamoto, K., Yada, T., Nishimura, M., Nakato, A., Miyazaki, A., Yogata, K., Abe, M., Okada, T., Usui, T., Yoshikawa, M., Saiki, T., Tanaka, S., Terui, F., Nakazawa, S., Watanabe, S.-i., Tsuda, Y. and Hayabusa2-initial-analysis, SOM Team. (2023) Uracil in the carbonaceous asteroid (162173) Ryugu. *Nature Communications*. **14**, 1292.
- Okazaki, R., Marty, B., Busemann, H. *et al.* (2023) Noble gases and nitrogen in samples of asteroid Ryugu record its volatile sources and recent surface evolution. *Science*. **379**, eabo431.
- Palme, H. and Zipfel, J. (2022) The composition of CI chondrites and their contents of chlorine and bromine: Results from instrumental neutron activation analysis. *Meteorit. Planet. Sci.* **57**, 317-333.
- Paquet, M., Moynier, F., Yokoyama, T. *et al.* (2023) Contribution of Ryugu-like material to Earth's volatile inventory by Cu and Zn isotopic analysis. *Nature Astronomy*. **7**, 182-189.
- Scott, E. R. D. and Krot, A. N. (2014) 1.2 - Chondrites and Their Components. *Treatise on Geochemistry (Second Edition)* (Holland, H. D. and Turekian, K. K. eds.), 65-137, Elsevier.
- Schönbächler, M. *et al.* Zirconium isotope composition indicate s-process depletion in samples returned from asteroid Ryugu. *Meteorit. Planet. Sci. in revision*
- Tachibana, S., Abe, M., Arakawa, M., Fujimoto, M., Iijima, Y., Ishiguro, M., Kitazato, K., Kobayashi, N., Namiki,

- N. and Okada, T. (2014) Hayabusa2: Scientific importance of samples returned from C-type near-Earth asteroid (162173) 1999 JU3. *Geochem. J.* **48**, 571-587.
- Tachibana, S., Sawada, H., Okazaki, R. *et al.* (2022) Pebbles and sand on asteroid (162173) Ryugu: In situ observation and particles returned to Earth. *Science*. **375**, 1011-1016.
- Torrano, Z. A., Jordan, M. K., Mock, T. D. *et al.* (2024) Neodymium-142 deficits and samarium neutron stratigraphy of C-type asteroid (162173) Ryugu. *Meteorit. Planet. Sci.* in press.
- Yada, T., Abe, M., Okada, T. *et al.* (2022) Preliminary analysis of the Hayabusa2 samples returned from C-type asteroid Ryugu. *Nature Astronomy*. **6**, 214-220.
- Yokoyama, T., Nagashima, K., Nakai, I. *et al.* (2023a) Samples returned from the asteroid Ryugu are similar to Ivuna-type carbonaceous meteorites. *Science*. **379**, eabn7850.
- Yokoyama, T. and Tsujimoto, T. (2021) Nucleosynthesis: The Where and How. *Encyclopedia of Geology (Second Edition)* (Alderton, D. and Elias, S. A. eds.), 1-19, Academic Press.
- Yokoyama, T., Wadhwa, M., Iizuka, T. *et al.* (2023b) Water circulation in Ryugu asteroid affected the distribution of nucleosynthetic isotope anomalies in returned sample. *Science Advances*. **9**, eadi7048.